III. CONCLUSIONS

Thus, it was found that, in contrast to the one-step application of the perovskite precursor and drying of the perovskite film at room temperature, the two-step SSE method makes it possible to improve the crystal structure of thin perovskite films. Due to overlapping of the two layers of the film, porosity is reduced and there are no through holes that short-circuit the functional layers of the photovoltaic cell. Moreover, the annealing promotes consolidation and packing of film grains.

REFERENCES

[1] Park, N.G. Organometal perovskite light absorbers toward a 20% efficiency low-cost solid-state mesoscopic solar cell // J. Phys. Chem. Lett. – 2013. – Vol. 4. – P. 2423-2430.

[2] Zhou Y., Yang M., Wu W., Vasiliev A. L., Zhu K., Padture N. P. Room-Temperature Crystallization of Hybrid-Perovskite Thin Films via Solvent-Solvent Extraction for High-Performance Solar Cells // J. Mater. Chem. A. – 2015. – Vol. 15. – P.1–18.

THE EXCITATION POWER DEPENDENCE OF THE RAMAN G AND 2D PEAKS OF SUSPENDED GRAPHENE GROWN BY CHEMICAL VAPOR DEPOSITION

K. Nigerish, M. Mikhalik, N. Kovalchuk, I. Komissarov
Belarusian State University of Informatics and Radioelectronics, Minsk, Belarus

I. INTRODUCTION

Increasing the power densities of electronic device makes the problem of an efficient heat removal crucial for their performance. High electron mobility transistors (HEMT) based on GaN provide an order of magnitude higher power densities than GaAs based transistors do [1]. In such high-power density devices the hot spots formed by non-uniform heat generation significantly reduce devices efficiency [2]. Balandin and co-authors showed that graphene quilts can be used for thermal management of GaN HEMTs [3]. Indeed, graphene has exceptional thermal conductivity [4], but its value strongly varies with defects density [5], number of layers and their stacking order [6]. The heat conductivity measurement of graphene is itself a challenging task. One of the most common methods to measure thermal transport in graphene (or in 2D materials in general) is optothermal Raman thermometry [4, 7]. The ideology of these experiments is based on the opportunity to heat graphene and measure its temperature simultaneously at the same point by the laser beam, where the positions of G and 2D peaks are used to trace the temperature rise.

In this article we present the results of the excitation power dependence study of the Raman G and 2D peaks of graphene grown by chemical vapor deposition and suspended over copper grid with 100 μm diameter holes.

II. SYNTHESIS AND TRANSFER OF GRAPHENE

The synthesis of graphene was carried out by atmospheric pressure chemical vapor deposition (APCVD). This process is described in more detail in work [8]. In this work, we employed a wet-chemical room temperature transfer process of graphene. The copper foil was totally dissolved in a water solution of $FeCl_3$. The graphene film was gently washed several times in a bath with distilled water prior to the transfer onto copper grid, which includes through holes.

III. EXPERIMENT

Raman spectra were recorded using Confotec NR500 confocal micro-Raman spectrometers, with 473 nm excitation wavelength. Micro Raman spectrometer mapping, 20x20 μm^2, procedure was performed with 1 μm step and beam size spot ≈ 600 nm. The scheme of Raman experiment is presented in Figure 1. The transferred procedure leads about 10 % of holes coverage. The Figure 2 demonstrates optical and Raleigh images of suspended graphene which fully covers the hole in the grid. It is clearly seen that the graphene morphology is non homogeneous (light and dark spots) which are related to the thicker and thinner parts of the film [9]. Taking in the account the observed non-homogeneity we have decided instead to study Raman spectra locally perform mapping of the central part of the suspended graphene and study how the distributions of G and 2D bands positions change with the power of the laser beam. In the course of the

experiment, the sample was scanned in the same region with different laser excitation powers: 145 μW, 565 μW, 910 μW and 1450 μW.

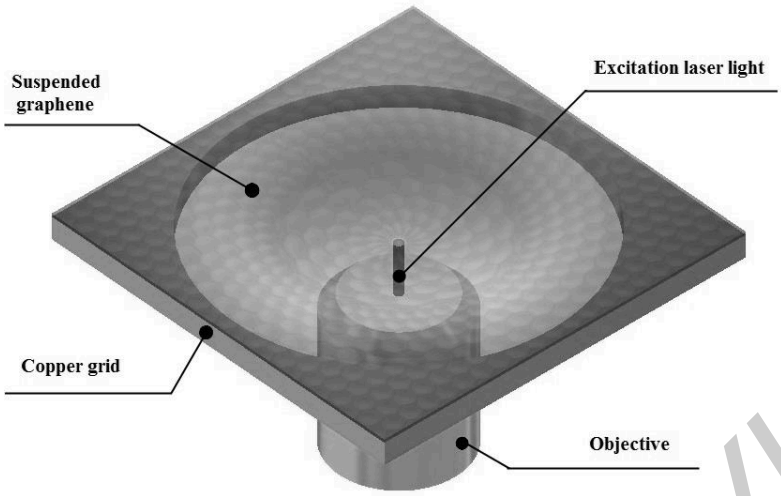

Figure 1 – The scheme of the experiment

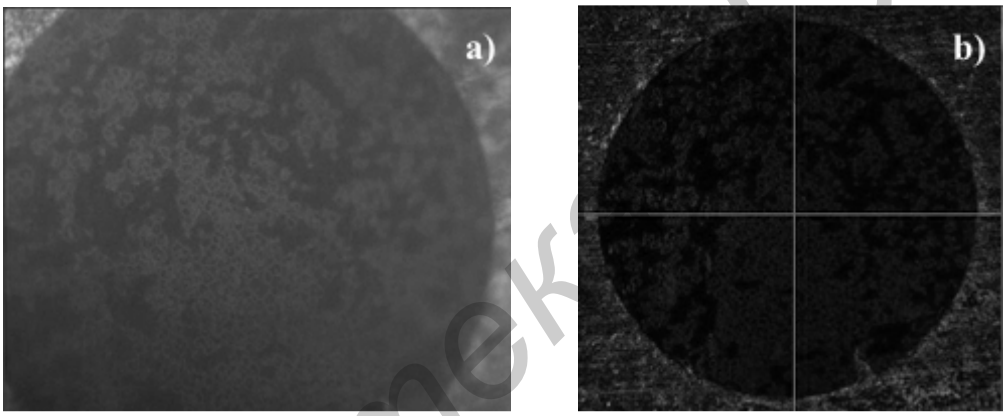

Figure 2 – The top view suspended graphene over 100 μm hole in copper grid a) optical image and b) Raleigh image

IV. RESULTS AND DISCUSSION

The results of this study are presented in figure 3, in which we show the distributions of G band (Figure 3 a) and 2D band (Figure 3 b) positions taken from Raman mapping data recorded with 145 μW and 1450 μW (the distribution for 565 μW and 910 μW is not built due to overlap with a distribution of 145 μW and 1450 μW, respectively).

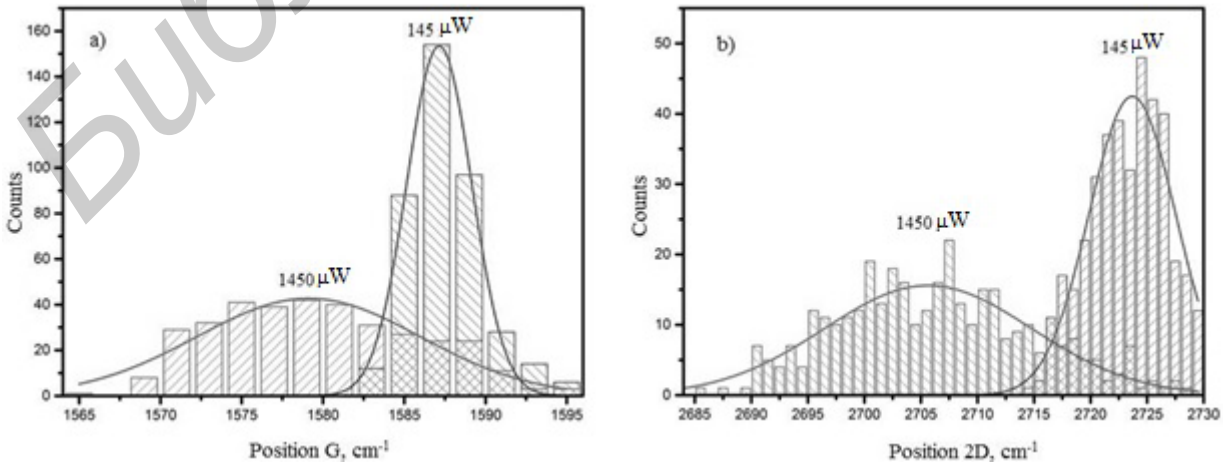

Figure 3 – The distribution histograms of G peaks a) and 2D peaks b). The solid lines are Gaussian fits

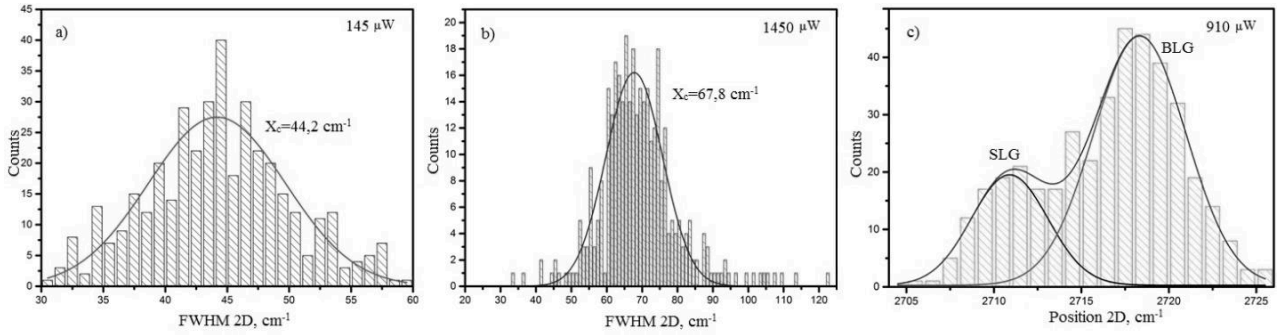

Figure 4 – The distribution histograms of 2D peaks a) FWHM 2D (laser excitation power 145 μW) b) FWHM 2D (laser excitation power 1450 μW) c) Position 2D (laser excitation power 910 μW). The solid lines are Gaussian fits data points

From Raman spectroscopy results presented in the Figure 4 it was found that a non-monotonic distribution was inherent for almost all data histograms. For example, two sharp maxima are observed in the position of the 2D band histogram (Figure 4 c). This suggests that within the same film there are at least two graphene ”systems” with quite different numbers of layers. Consequently, it is reasonable to analyze Raman spectra separately applying the criterion for data belonging to a particular peak. Following this idea, we split the Raman data of graphene film into two sets, one of which we attribute to a single layer graphene (SLG) and another which contains data specific for bilayer graphene [8].

We plot the positions of the maxima of the experimental distributions as a function of the laser power (Figure 5). According to the linier fit of the experimental dependences the values for the slope are ≈0,0035 $cm^{-1}/\mu W$ for G band and ≈ 0,0134 $cm^{-1}/\mu W$ for 2D band of SLG and ≈ 0,0134 $cm^{-1}/\mu W$ for 2D band of BLG, respectively.

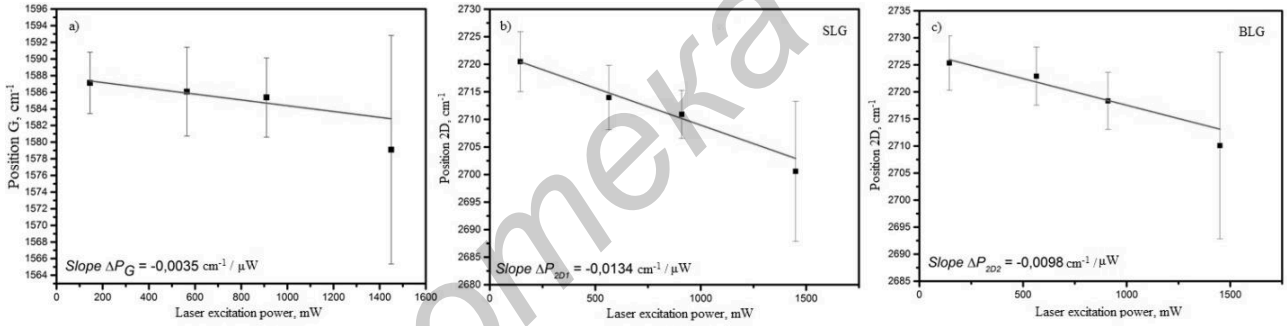

Figure 5 – The linear fit of the power dependence of G a) and 2D SLG b), 2D BLG c) peaks positions.
The experimental points and error bars correspond to the maxima and widths of fitting Gaussians (see Figure 3).

The presented scheme of the experiment is widely used in the experiments for heat conductivity measurements [7]. From mathematical point of view the circular symmetry of the experiment is the additional advantage since its left only one independent variable in the heat diffusion equation. For that reason, in all these experiments the Raman spectra of graphene are recorded at the center of suspended graphene. In our experiment the value of the ratio $D_{hole}/dS_A \approx 4$, where Dhole – the diameter of the hole, dS_A- diagonal of the scanned area, allows us, at the fist approach, to consider any point within the scanned area as the central one, meaning that for every single Raman spectrum measurement the circular symmetry of the experiment is preserved. Therefore, the obtained results can be used to estimate the value of heat conductivity. However, the temperature dependence of Raman peaks position has to be measurement for this purpose, as shown in [6].

V. CONCLUSION

Finally, in our work we successfully transferred graphene grown by CVD over copper grid with 100 μm holes. The power dependence of G and 2D Raman bands position distributions were measured with 473 nm excitation laser in 145-1450 μW range. The linear fit of the experimental data gives values of power slopes ≈ 0,0035 $cm^{-1}/\mu W$ for G band and ≈ 0,0134 $cm^{-1}/\mu W$ for 2D band of SLG and ≈ 0,0134 $cm^{-1}/\mu W$ for 2D band of BLG, respectively.

REFERENCES

[1] Faqir M., Batten T., Mrotzek T., Knippscheer S., Massiot M., Buchta M., Blanck H., Rochette S., Vendier O. and Kuball M. Microelectronics Reliability. 52, 3022 (2012).
[2] Sarua A., Ji H., Kuball M., Uren M. J., Martin T., Hilton K. P. and Balmer R. S. IEEE Transactions on Electron Devices. 53, 2438 (2006).
[3] Yan Z., Liu G., Khan J. M., and Balandin A. A. Nature communications. 3, 827 (2012).
[4] Balandin A. A., Ghosh S., Bao W., Calizo I., Teweldebrhan D., Miao F. and Lau C. N. Nano letters. 8(3), 902 (2008).
[5] Malekpour H., Ramnani P., Srinivasan S., Balasubramanian G., Nika D., Mulchandani L. and Balandin A. A. Nanoscale. 8(30), 14608 (2016).
[6] Li H., Ying H., Chen X., Nika D. L., Cocemasov A. I., Cai W., Balandin A. A. and Chen S. Nanoscale. 6, 13402 (2014).
[7] J. Lee J-U, Yoon D., Kim H., Lee S. W., and Cheong H. Phys. Rev. B 83, 081419(R) (2011).
[8] I. V. Komissarov, N. G. Kovalchuk, V. A. Labunov, K. V. Girel, O. V. Korolik, M. S. Tivanov, A. Lazauskas, M. Andrulevičius, T. Tamulevičius, V. Grigaliūnas, Š. Meškinis, S. Tamulevičius, S. L. Prischepa. Beilstein Journal of Nanotechnology, 8, (2017).
[9] Komissarov I. V., Kovalchuk N. G., Kolesov E. A., Tivanov M. S., Korolik O. V., Mazanik A. V., Shaman Yu. P., Basaev A. S., Labunov V. A., Prischepa S. L., Kargin N. I., Ryzhuk R. V., Shostachenko S. A. Physics Procedia. 72, 450 (2015).

OPTICAL COUPLING OF SILICON CHIPS BY MICROCHANNEL VIAS INTERPOSER

S. Lazarouk[1], A. Leshok[1], A. Dolbik[1], Le Dinh Vi[1], T. Kozlova[1], V. Vysotskii[2], S. Shvedov[2], V. Saladukha[2], V. Labunov[1]
[1] Belarusian State University of Informatics and Radioelectronics, Minsk, Belarus
[2] Joint Stock Company “INTEGRAL”, Minsk, Belarus

I. INTRODUCTION

The performance increase is currently one of the main tasks of the integrated electronics development. Replacement of electronic interconnects to optical ones will improve the performance of integrated circuits (ICs) by eliminating the resistive-capacitive delay of the metal wiring. A significant expectations are connected with the silicon based optical interconnects implemented in the form of optocouples which includes Si light emitting sources and photoreceivers connected by the waveguides of different constructions. Among the advantages of such a system is its compatibility with the highly developed mass production CMOS technology. Classical approach in optocouple designing is that all three main elements such as light-emitting diode (LED), photodiode (PD), and waveguide (WG) are located in a horizontal plane [1-3]. Recently a new technology was proposed and now it is in intensive development.

We have developed and manufactured a system that provides optical interconnects between silicon chips based on silicon avalanche LEDs and silicon microchannel plate vias. Measurements showed a reproducible response of the optical signal of the avalanche LEDs registered by photodiodes on a silicon chip, which has no electrical commutation to another silicon chip on which the sources of the optical signal are located.

II. EXPERIMENTAL

Silicon chips were produced by the conventional CMOS technology. N-type monocrystalline silicon with a resistivity of 0.3 Ω·cm was used as initial substrate. SiO_2 layer of 0.8 μm thickness was formed on the silicon surface by thermal oxidation and regular windows were open in this layer by plasma etching. Then the aluminum/silicon composite film of 0.1 μm thickness was deposited over the SiO_2 layer by magnetron sputtering of aluminum/silicon alloy target with the Si content of 30 at. %. As a result, a composite film with Si nanoparticles embedded into Al host is formed [4]. After that a pure aluminum film of 1 μm thickness was deposited over the composite film.

The deposited films were subjected to anodic treatment in a 20 % aqueous solution of phosphoric acid via preformed photoresist masks at their surfaces. Such treatment led to the oxidation of the deposited films in unmasked areas. It's known that aluminum and silicon have the various velocities of oxidation. Therefore the anodic treatment of Al/Si film resulted in formation of nanostructured composite material, containing clusters of slightly oxidized nanoparticles of Si embedded into the alumina matrix [4]. Not